

Electronic Supplementary Information

Construction of strongly coupled 2D-2D SnS₂/CdS S-Scheme heterostructures for photocatalytic hydrogen evolution

Xiaoyu Chen, Zhi Han, Zonghao Lu, Tingting Qu, Ce Liang, Yu Wang, Bin Zhang*, Xijiang Han*,
and Ping Xu*

MIIT Key Laboratory of Critical Materials Technology for New Energy Conversion and Storage, School of
Chemistry and Chemical Engineering, Harbin Institute of Technology, Harbin 150001, China. Email:
pxu@hit.edu.cn (P.X.); hanxijiang@hit.edu.cn (X.H.); zhangbin_hit@aliyun.com (B.Z.)

Contents

Fig. S1	PerfectLight Labsolar 6A and PerfectLight PLS-SXE300/300UV.
Fig. S2	Optical photos of CdS nanosheets, 2D-2D SnS ₂ /CdS heterostructures and SnS ₂ nanosheets.
Fig. S3	SEM image of pure SnS ₂ nanosheets.
Fig. S4	Nitrogen sorption isotherms and the corresponding Barrett-Joyner-Halenda (BJH) pore size distribution plots of pure SnS ₂ nanosheets.
Fig. S5	XPS survey spectra of SnS ₂ /CdS and pure CdS.
Fig. S6	XPS survey spectra and S 2p XPS peaks of pure SnS ₂ nanosheets.
Fig. S7	UV-vis absorption spectrum and optical band gap of pure SnS ₂ .
Fig. S8	Time-resolved transient photoluminescence decay spectra of the pure SnS ₂ nanosheets.
Fig. S9	XRD pattern, Sn 3d XPS peaks, Cd 3d XPS peaks, and S 2p XPS peaks of SnS ₂ /CdS heterostructures before and after reaction.
Fig. S10	EIS Nyquist plots, chronoamperometry curves, Mott-Schottky plots, linear sweep voltammogram curves of pure SnS ₂ nanosheets.
Fig. S11	XPS valance of (a) pure CdS and (b) pure SnS ₂ .
Fig. S12	models of CdS (002), SnS ₂ (100), and SnS ₂ /CdS heterostructures.
Fig. S13	charge density difference diagram of CdS (002), SnS ₂ (100), and SnS ₂ /CdS heterostructures.
Fig. S14	charge density diagram of CdS (002), SnS ₂ (100), and SnS ₂ /CdS heterostructures.
Table. S1	Time-resolved PL decay curve parameters obtained by double-exponential function simulation.
Table. S2	Photocatalytic hydrogen production performance (AQE) of photocatalysts reported in literatures.

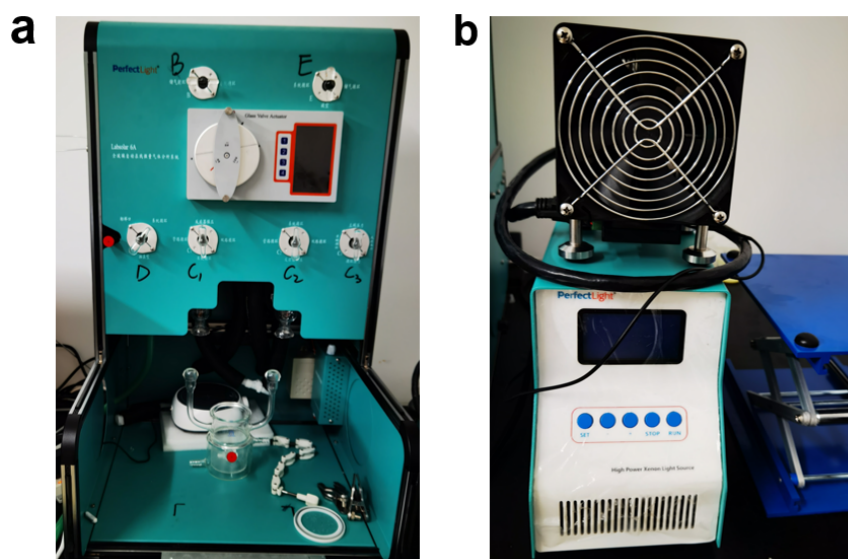


Fig. S1. (a) PerfectLight Labsolar 6A and (b) PerfectLight PLS-SXE300/300UV.

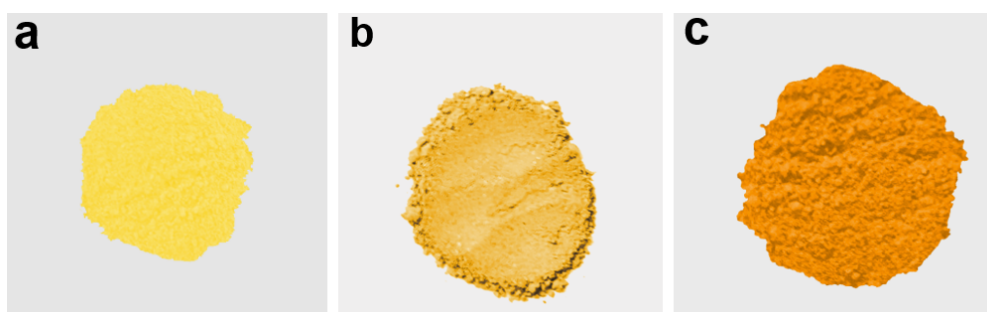


Fig. S2. Optical photos of (a) CdS nanosheets, (b) 2D-2D SnS₂/CdS heterostructures and (c) SnS₂ nanosheets.

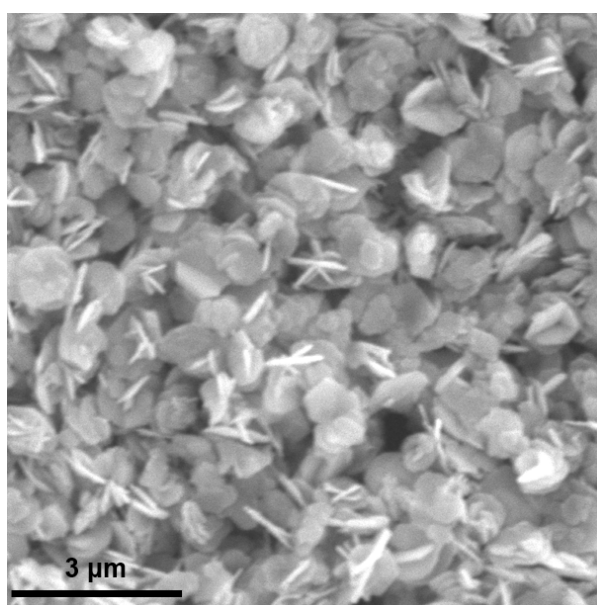


Fig. S3. SEM image of pure SnS₂ nanosheets.

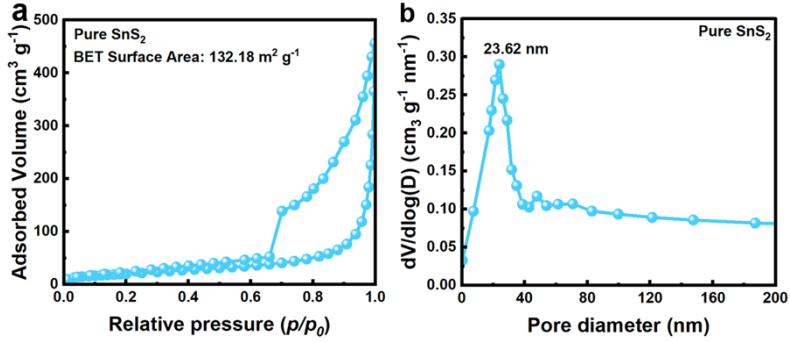


Fig. S4. Nitrogen sorption isotherms and the corresponding Barrett-Joyner-Halenda (BJH) pore size distribution plots of pure SnS₂ nanosheets.

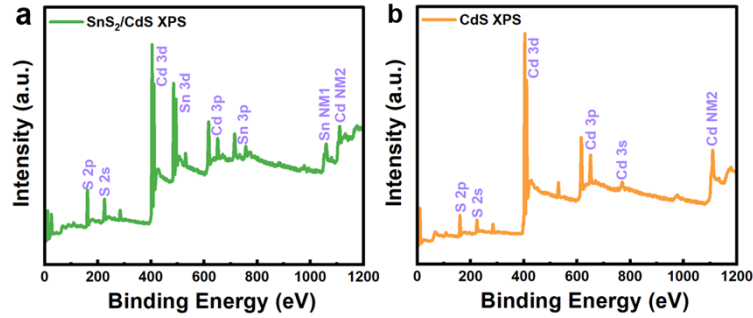


Fig. S5. XPS survey spectra of SnS₂/CdS and pure CdS.

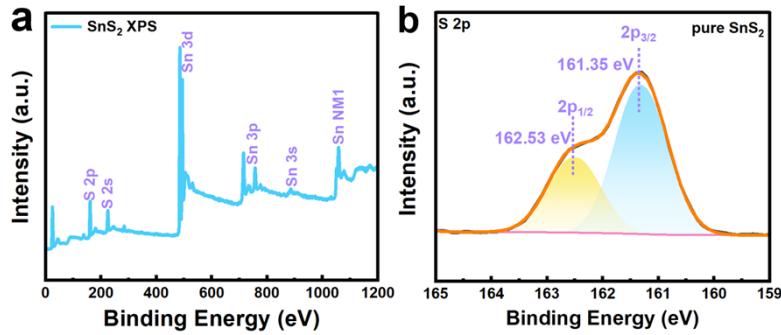


Fig. S6. XPS survey spectra and S 2p XPS peaks of pure SnS₂ nanosheets.

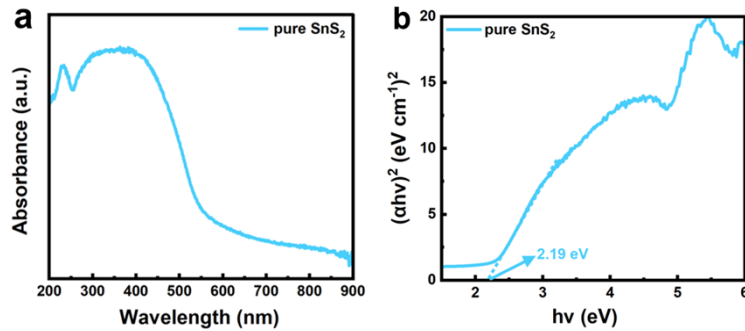


Fig. S7. (a) UV-vis absorption spectrum and (b) optical band gap of pure SnS₂.

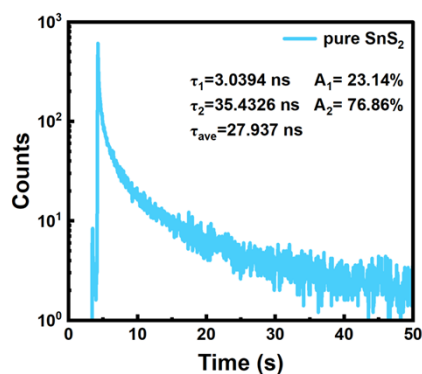


Fig. S8. Time-resolved transient photoluminescence decay spectra of the pure SnS₂ nanosheets.

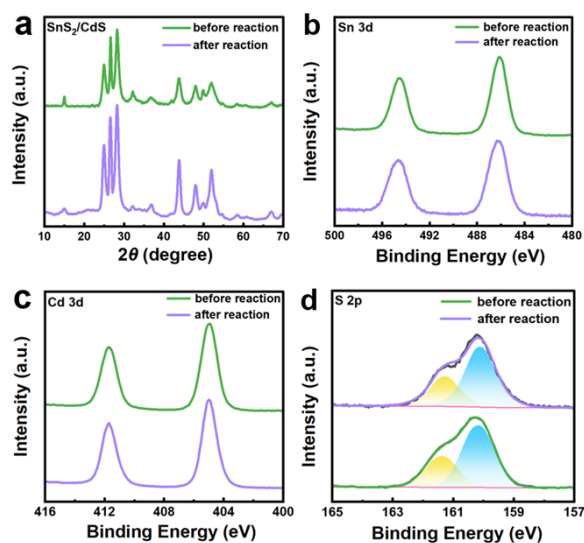


Fig. S9. (a) XRD pattern, (b) Sn 3d XPS peaks, (c) Cd 3d XPS peaks, and (d) S 2p XPS peaks of SnS₂/CdS heterostructures before and after reaction.

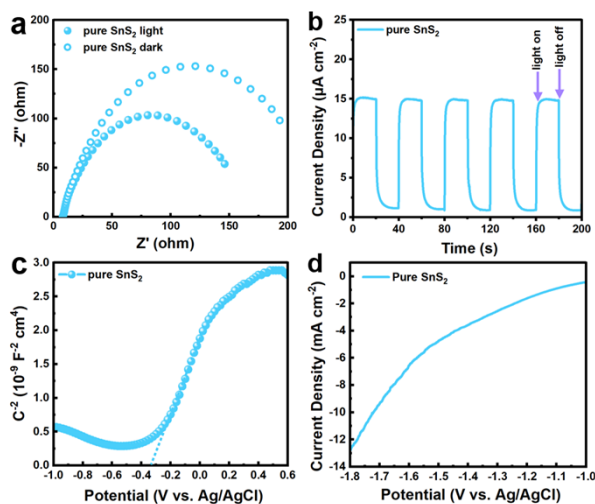


Fig. S10. (a) EIS Nyquist plots, (b) chronoamperometry curves, (c) Mott-Schottky plots, (d) linear sweep voltammogram curves of pure SnS₂ nanosheets.

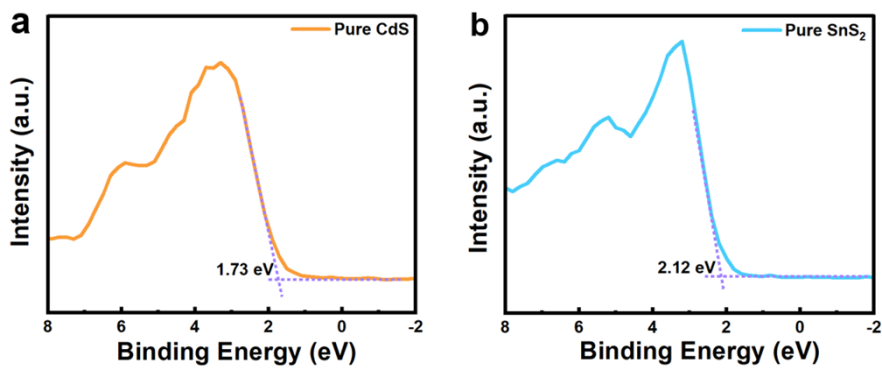


Fig. S11. XPS valance of (a) pure CdS and (b) pure SnS₂.

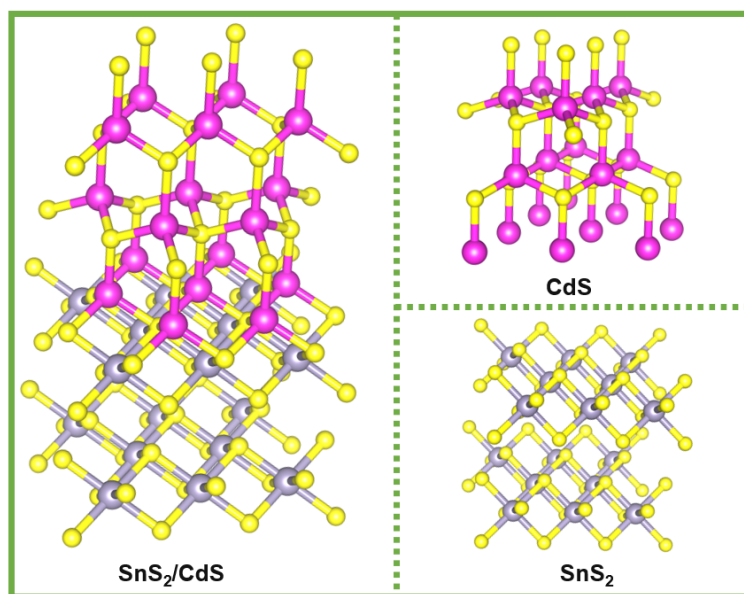


Fig. S12. models of CdS (002), SnS₂ (100), and SnS₂/CdS heterostructures.

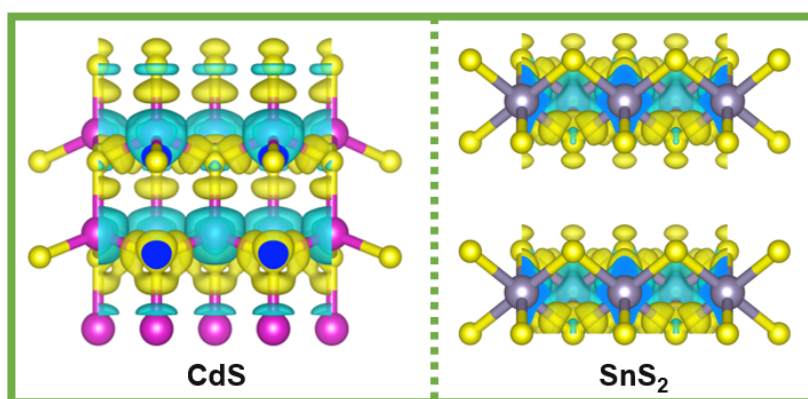


Fig. S13. charge density difference diagram of CdS (002), SnS₂ (100), and SnS₂/CdS heterostructures.

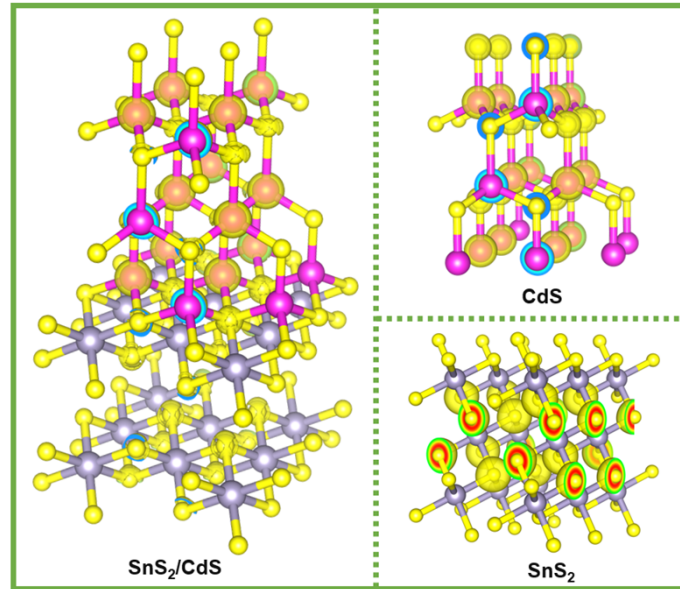


Fig. S14. charge density diagram of CdS (002), SnS₂ (100), and SnS₂/CdS heterostructures.

Table S1. Time-resolved PL decay curve parameters obtained by double-exponential function simulation.

samples	τ_1 (ns)	τ_2 (ns)	A_1 (%)	A_2 (%)	τ_{ave} (ns)
CdS	0.8202	3.8416	67.53	32.47	1.80
SnS ₂ /CdS	1.3303	3.7453	67.17	32.83	2.12
SnS ₂	3.0394	35.4326	23.14	76.86	27.94

Table S2. Photocatalytic hydrogen production performance (AQE) of photocatalysts reported in literatures.

Photocatalysts	AQE (420 nm)	Noble metal	Sacrificial agent	Ref.
CdS/RGO	22.5%	0.5 wt% Pt	10 wt% lactic acid solution	1
CdS/ZnS	9.3%	none	0.5 M Na ₂ S and 0.5 M Na ₂ SO ₃	2
MoS ₂ /CdS	14.7%	none	10 wt% lactic acid solution	3
CdS/TiO ₂	11.9%	0.5 wt% Pt	0.35 M Na ₂ S and 0.25 M Na ₂ SO ₃	4
FeP/CdS	11.2%	none	10 wt% lactic acid solution	5
CuS/CdS	19.7	none	10 wt% lactic acid solution	6
PtNi _x /CdS	51.2%	2 wt% Pt	0.35 M Na ₂ S and 0.25 M Na ₂ SO ₃	7
CdS/WS ₂ /graphene	21.2%	none	0.35 M Na ₂ S and 0.25 M Na ₂ SO ₃	8
Ni ₂ P/MCdS-DETA	26.4%	none	0.35 M Na ₂ S and 0.25 M Na ₂ SO ₃	9
CDs/CdS-S	11.8%	none	10 wt% lactic acid solution	10
SnS₂/CdS	59.3	none	10 wt% lactic acid solution	This work

Reference

1. Q. Li, B. Guo, J. Yu, J. Ran, B. Zhang, H. Yan and J. Gong, Highly efficient visible-light-driven photocatalytic hydrogen production of CdS-cluster-decorated graphene nanosheets, *J. Am. Chem. Soc.*, 2011, **133**, 10878-10884.
2. Y. Lin, Q. Zhang, Y. Li, Y. Liu, K. Xu, J. Huang, X. Zhou and F. Peng, The evolution from a typical type-I CdS/ZnS to type-II and Z-scheme hybrid structure for efficient and stable hydrogen production under visible light, *ACS Sustainable Chem. Eng.*, 2020, **8**, 4537-4546.
3. A. Wu, C. Tian, Y. Jiao, Q. Yan, G. Yang and H. Fu, Sequential two-step hydrothermal growth of MoS₂/CdS core-shell heterojunctions for efficient visible light-driven photocatalytic H₂ evolution, *Appl Catal B*, 2017, **203**, 955-963.
4. Z. Jiang, K. Qian, C. Zhu, H. Sun, W. Wan, J. Xie, H. Li, P. K. Wong and S. Yuan, Carbon nitride coupled with CdS-TiO₂ nanodots as 2D/0D ternary composite with enhanced photocatalytic H₂ evolution: A novel efficient three-level electron transfer process, *Appl Catal B*, 2017, **210**, 194-204.
5. K. Sun, J. Shen, Y. Yang, H. Tang and C. Lei, Highly efficient photocatalytic hydrogen evolution from 0D/2D heterojunction of FeP nanoparticles/CdS nanosheets, *Appl Surf Sci*, 2020, **505**, 144042.
6. F. Zhang, H. Q. Zhuang, W. Zhang, J. Yin, F. H. Cao and Y. X. Pan, Noble-metal-free CuS/CdS photocatalyst for efficient visible-light-driven photocatalytic H₂ production from water, *Catal. Today*, 2019, **330**, 203-208.
7. Q. Ba, X. Jia, L. Huang, X. Li, L. Gao and L. Mao, Hollow structured PtNi alloy as cocatalyst of CdS for hydrogen generation under visible light irradiation, *Int J Hydrogen Energy*, 2019, **44**, 28104-28112.
8. Q. Xiang, F. Cheng and D. Lang, Hierarchical layered WS₂/graphene modified CdS nanorods for efficient photocatalytic hydrogen evolution, *ChemSusChem*, 2016, **9**, 996-1002.
9. T. Hu, K. Dai, J. Zhang, G. Zhu and C. Liang, Noble-metal-free Ni₂P as cocatalyst decorated rapid microwave solvothermal synthesis of inorganic-organic CdS-DETA hybrids for enhanced photocatalytic hydrogen evolution, *Appl Surf Sci*, 2019, **481**, 1385-1393.
10. C. Zhu, C. Liu, Y. Fu, J. Gao, H. Huang, Y. Liu and Z. Kang, Construction of CDs/CdS photocatalysts for stable and efficient hydrogen production in water and seawater, *Appl Catal B*, 2019, **242**, 178-185.